

Supporting information for: Engineering biosensors with extended, narrowed, or arbitrarily edited dynamic range

Alexis Vallée-Bélisle, Francesco Ricci & Kevin W. Plaxco

I-SUPPORTING METHODS

HPLC purified molecular beacons modified with a 5'-FAM and a 3'-BHQ-1, and samples of the 13 nucleotide targets (perfect match and mismatch) were purchased from Sigma-Genosys (see Figure S1). All experiments were conducted at pH 7.0 in 50 mM sodium phosphate buffer, 150 mM NaCl, at 45°C. All fluorescence measurements were obtained using a Cary Eclipse Fluorimeter with excitation at 480 (± 5) nm and acquisition between 514 and 520 nm.

Binding curves for individual sensors (Figure 2b-c) were obtained using 5 nM of molecular beacon by sequentially increasing the target concentration (perfect match or mismatch) via the addition of small volumes of solutions with increasing concentration of target that also contain similar concentration of molecular beacon concentration. Individual binding curves were fitted to a single-site binding mechanism ($[T]$ = target concentration; Amp = fluorescence amplitude; F_0 = background fluorescence):

$$F_{[T]} = F_0 + \left(\frac{[T](Amp)}{[T] + K_D} \right) \quad (\text{Eq. 1})$$

Extended and edited binding curves (Figure 3b) were obtained using the optimal mixtures predicted by our simulations (Figure S4) and a total molecular beacons concentration of 10nM (20 nM for the sensor with four receptors). Sensor mixture containing two (or four) sensors were fitted to the simulated function representing the sum of two (or four) individual sensor (Eq. 2) using the known dissociation constant (K_D), and the fluorescence amplitude expected from each molecular beacon (determined from the proportion of each molecular beacon and its relative fluorescence amplitude –see Figure S4).

$$F_{[T]} = F_0 + \left(\frac{[T](Amp^1)}{[T] + K_D^1} \right) + \left(\frac{[T](Amp^2)}{[T] + K_D^2} \right) + (\dots) \quad (\text{Eq. 2})$$

Narrowed dynamic range sensors (Figure 4b-c) were obtained using solutions of 10 nM of 1GC molecular beacons by varying the concentration of the depletant molecule (non-switching, non-signaling recognition element –see Figure S1b). The resulting data were fitted to the Hill equation, which is used to describe ultrasensitive systems in biochemistry (H = Hill coefficient)³⁷.

$$F_{[T]} = F_0 + \left(\frac{[T]^H (Amp)}{[T]^H + K_D} \right) \quad (\text{Eq. 3})$$

II- TABLE S1

Switching thermodynamics (K_S), affinities (K_D), total fluorescence change and gain of the various stem-loops.

# of GC in the 5 base-pairs stem	K_S^a	K_d (μM) ^a	Total fluo. change ^b	Gain ^c
0GC	1.1	0.012 (± 0.001)	0.48	0.9
1GC	0.2	0.044 (± 0.004)	0.83	4.9
2GC	0.05	0.250 (± 0.02)	0.95	19
3GC	0.01	4.4 (± 0.4)	1	>20
4GC	0.001	28 (± 1)	1	>20
5GC	0.00006	128 (± 9)	1	>20

^a Values are for the FAM/BHQ-1 modified molecular beacons. K_S is the equilibrium constant for the conformational switch and K_D is the dissociation constant for a 13-base perfect match target¹⁹. Total fluorescence change (relative to 1, the maximal fluorescence change possible)^b and gain^c of each fluorescent receptor. Switches with K_S higher than 0.01 will display lower fluorescence change and lower gain since a greater fraction of these receptors populate the signal “on” state in the absence of target (see Figure S4). Total fluorescence change = $1 - K_S / (1 + K_S)$. Gain = Total fluorescence change / (1 - Total fluorescence change).

III-SUPPORTING FIGURES

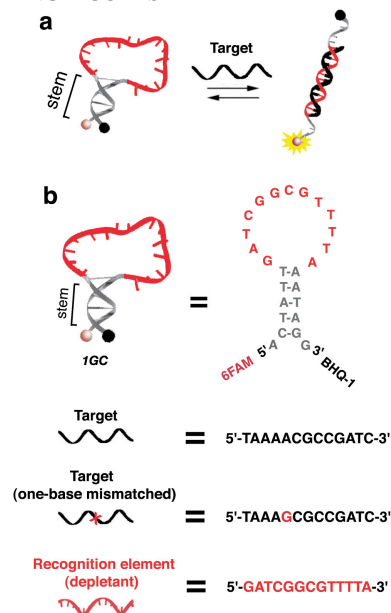


Figure S1. Molecular beacons, targets and depletant. (a) Via the addition of a fluorophore/quencher pair at the extremities of the stem, DNA stem-loop sequences are easily converted into efficient fluorescent sensors termed molecular beacons³. (b) Shown is the nucleotide sequence of the molecular beacon denoted 1GC (containing one GC base pair in the five base pair stem) in this work, its DNA target, the one-base mismatched target, and the DNA recognition element (depletant) used in here (Figure 4).

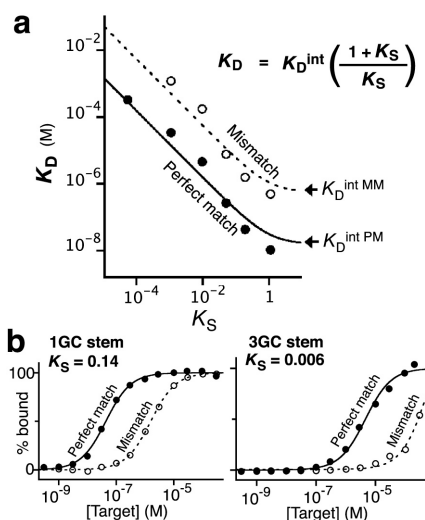


Figure S2. (a) Quantitative correlation between the affinity of a receptor for its target (K_D) and its switching equilibrium constant (K_S). We can arbitrarily reduce the affinity of a receptor for its target by introducing a switching mechanism, and then tuning the switching equilibrium constant, K_S .²¹ Under these circumstances, the modifications that modulate K_S are far from the binding interface and thus do not affect receptor specificity. (b) Such modification generally does not alter the receptor's binding interface (see Figure 2) and does not alter specificity. This is demonstrated here by comparing the difference in affinity displayed by receptor 1GC and 3GC for a perfectly matched (PM) target and a one-base mismatched (MM) target. The nearly identical offset between the PM and MM curves illustrate the identical specificity profiles of the two receptors (see also affinity of our six receptor variants for the one-base mismatch in (a)). The average difference in affinity between the perfect match (PM) and one-base mismatch (MM) is 35(\pm 4)-fold.

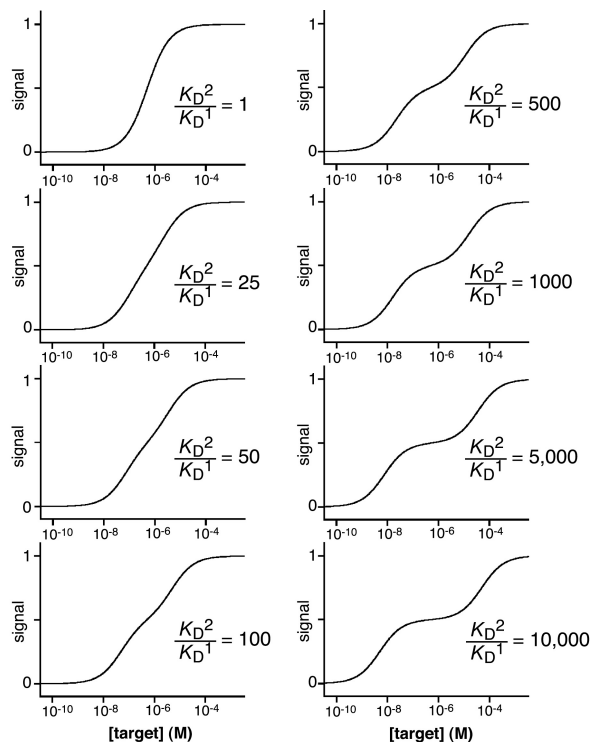


Figure S3. Simulated outputs of sensors composed of equimolar concentrations of two receptors with affinities differing by K_D^2 / K_D^1 . The dynamic range of sensors can be extended by approximately 2 orders of magnitude by combining two receptors differing in affinity by ~ 2 orders of magnitude ($K_D^2 / K_D^1 = 100$). Combinations of receptors that differ by more than 500-fold in affinity produce more complex ‘three-state’ dose-response sensors, which ‘push’ their useful dynamic range towards extreme conditions at the cost of poorer sensitivity at intermediate concentrations.

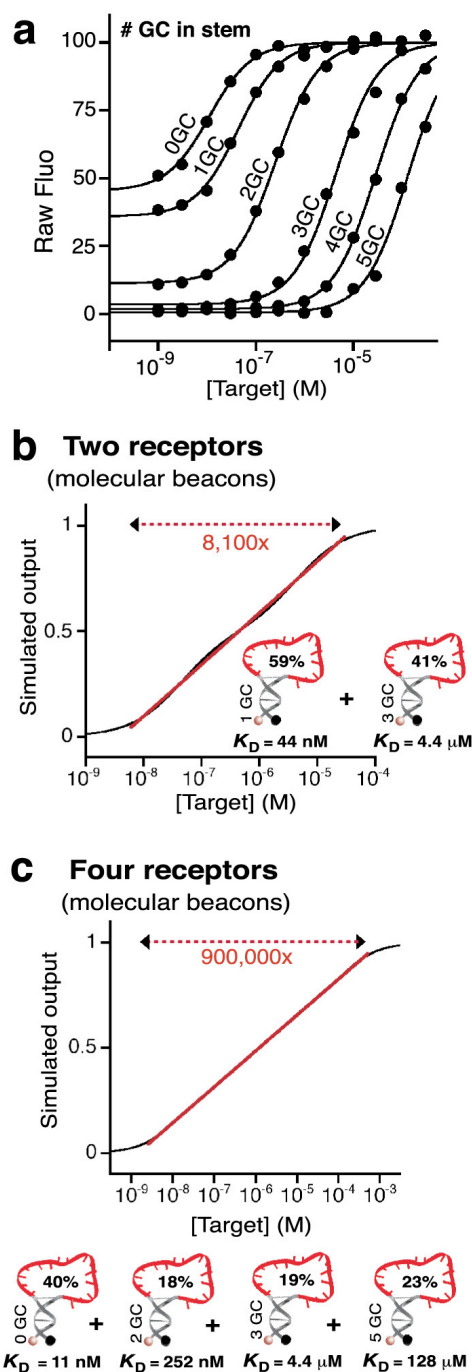


Figure S4. Predicting the optimal receptor composition needed to create sensors with widest, log-linear dynamic ranges. (a) The total fluorescence change provided by a structure-switching receptor is a function of its switching equilibrium constant, K_s ¹⁹. For example, a molecular beacon with a switching equilibrium constant of ~ 1 (e.g. 0GC –see Table S1) produces a significant fluorescent background because $\sim 50\%$ of the structure is open even in the absence of target. This leads to a reduced fluorescence change upon target saturation (Table S1)¹⁹. (b) Molecular beacons 1GC and 3GC exhibit the ideal 100-fold variation in their affinity in order to create a sensor with a log-linear dynamic range of 8,100-fold (see Figure S3). Using the known dissociation constants and relative fluorescence change of these two receptors (Table S1), we are able to find the ratiometric mixture that enables the best fit to a log-linear function (eq. 2). (c) A similar procedure is used to predict the optimal mixture ratios of

molecular beacons 0GC, 2GC, 3GC and 5GC (40/18/19/23) to produce a dynamic range spanning a 900,000-fold range of target concentrations. Again, a larger proportion of beacon 0GC is required in the mixture in order to account for the smaller fluorescence change produced by this molecular beacon (see a). With the smaller fluorescence change provided by molecular beacons 0GC and 1GC (48% and 83% of the maximum possible fluorescent change –Table S1), the fluorescence changes of the “mixed” sensors 1GC-3GC and 0GC-2GC-3GC-5GC are thus 90% and 78% that of the maximal fluorescence change possible, respectively (gains of 9-fold and 3.6-fold).

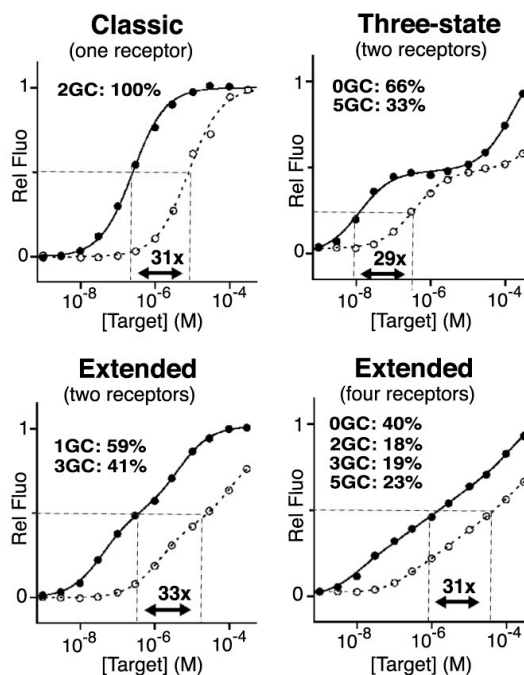


Figure S5. By employing a structure-switching mechanism to tune the affinities of our receptors we create sensors that maintain constant specificity profiles across their entire dynamic ranges. This is demonstrated by the close parallel between the sensors’ responses to perfectly matched (solid line) and single-base mismatched (dotted line) targets.

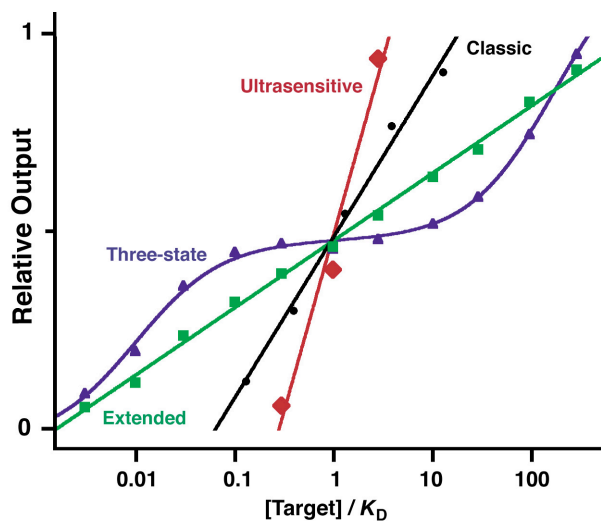


Figure S6. Editing the dynamic range of single-site receptors: summary of the dynamic ranges created in this study. (Black) Classic “single site” binding; (green) a sensor with extended dynamic range created by coupling four receptors; (red) an ultrasensitive sensor created via the sequestration mechanism; (blue) a three-state sensor created by combining two receptors differing significantly in affinity. For ease of comparison, the concentration at

mid-point of each sensor’s output curve (e.g., the dissociation constant for a single-site receptor) was set identical for each sensor ($[Target]/K_D$).

IV- SUPPORTING REFERENCE

(20) Dunker, A. K.; Lawson, J. D.; Brown, C. J.; Williams, R. M.; Romero, P.; Oh, J. S.; Oldfield, C. J.; Campen, A. M.; Ratliff, C. M.; Hipps, K. W.; Ausio, J.; Nissen, M. S.; Reeves, R.; Kang, C.; Kissinger, C. R.; Bailey, R. W.; Griswold, M. D.; Chiu, W.; Garner, E. C.; Obradovic, Z. *J Mol Graph Model* **2001**, *19*, 26-59.

(39) Hill, A. V. *J Physiol* **1910**, *40*: iv-vii.